The American Journal of Human Genetics, Volume *108*

Supplemental information

Bi-allelic premature truncating variants in *LTBP1* cause cutis laxa syndrome

Lore Pottie, Christin S. Adamo, Aude Beyens, Steffen Lütke, Piyanoot Tapaneeyaphan, Adelbert De Clercq, Phil L. Salmon, Riet De Rycke, Alper Gezdirici, Elif Yilmaz Gulec, Naz Khan, Jill E. Urquhart, William G. Newman, Kay Metcalfe, Stephanie Efthymiou, Reza Maroofian, Najwa Anwar, Shazia Maqbool, Fatima Rahman, Ikhlass Altweijri, Monerah Alsaleh, Sawsan Mohamed Abdullah, Mohammad Al-Owain, Mais Hashem, Henry Houlden, Fowzan S. Alkuraya, Patrick Sips, Gerhard Sengle, and Bert Callewaert

Supplemental Note: Case Reports

Family 1

Individual F1:II-2 is the daughter of a healthy consanguineous couple (first cousins) of Turkish origin. She was born at term after an unfollowed, but uneventful pregnancy by cesarean section. Birth weight was 3000g (P56; +0,16), length 50 cm (P58; +0,2SD). She presented with congenital diaphragmatic hernia (Morgagni) and bilateral inguinal hernia; the latter was corrected at age 6 months. At 12 months old, she was operated for the first time for the diaphragmatic hernia, but due to recurrence, surgery was repeated at the age of 18 months. Neuromotor development was normal. Clinical examination was at age 3 years and 4 months old showed mild cutis laxa and coarse craniofacial features, including a high forehead, frontal bossing, sagging cheeks, downslanted palpebral fissures, prominent supra-orbital ridges, a wide nasal bridge with broad nasal tip, long smooth philtrum, prominent nasolabial folds, and a broad mouth with thick lower lip vermillion. Several skeletal abnormalities were noticed, including short stature, ovoid-shaped vertebral bodies, brachydactyly, clinodactyly of the fifth finger, scoliosis, lumbar hyperlordosis, genua vara and joint hypermobility. X-ray images of the skull showed a copper beaten calvarium and a prominent coronal suture at the age of 3 years. Her height was 88 cm (P2; -2,19SD), her weight 12,450kg (P5; -1,38SD) and her OFC 50cm (P77; +0,72SD). Echocardiography showed mitral and tricuspid insufficiency with flattening of both valves during systole. Abdominal echography showed a caudally implanted and small right kidney. Vision and hearing were normal. Exome sequencing revealed the presence of a homozygous *LTBP1* frameshift variant (NM_206943.4: c.4844del (p.Asn1615Ilefs*23)).

Family 2

Family 2 consists of 4 affected individuals from two different couples from a large consanguineous family. Individual F2:V-3 is the third child from the first couple, who are first cousins through their mother and the father of the second family and second cousins through their father and the mother of the second family. Their first child died of an unknown cause. F2:V-3 was born after an uneventful pregnancy at 40 weeks of gestation. Her birth weight was 2520g (P4; -1,72SD), other anthropometric parameters were unknown. She presented with recurrent chest infections in the first few weeks of life and a diagnosis of cystic fibrosis was confirmed. Following referral to a geneticist at four months she was noted to have cutis laxa, craniosynostosis of the coronal sutures, short stature and craniofacial

dysmorphism. Facial features were overtly coarse and included a long face, sagging cheeks, downslanted palpebral fissures, prominent supraorbital ridges, proptosis, synophris and arch-shaped eyebrows. Eyelashes were strikingly long. She showed a prominent nose with convex nasal ridge, wide nasal bridge, broad nasal tip, long philtrum and thick lips. She had a cleft hard and soft palate. Other skeletal features included brachydactyly, 5th finger clinodactyly, syndactyly of the 2,3 and 4 toe and hip dislocation. She had bilateral inguinal hernia. Echocardiographic evaluation showed a mild concentric left ventricular hypertrophy. Neuromotor development was normal but she follows special education for learning difficulties. Mixed conductive and sensorineural hearing loss is present for which she has hearing aids. Ophthalmological evaluation showed the presence of hypermetropy. Additionally, she was diagnosed with myelofibrosis. Molecular analysis of the recurrent *FGFR3* Pro250Arg variant was normal. The youngest sibling, F2:V-4, was born after an uneventful pregnancy at 38 weeks of gestation and weighed 3000g. She presented with a squint at 15 months. Ophthalmological assessment revealed blindness secondary to optic nerve hypoplasia. She followed special education, had severe autism and no speech. She has mild conductive hearing loss. Craniofacial features included synophris, long eyelashes, a long face, thick lips, large nose and high (intact) palate. She had cutis laxa with a lax abdominal wall. She had no documented craniosynostosis, but clinically there was the impression of mild bitemporal narrowing. She had brachydactyly.

Individuals F2:V-8 and F2:V-9 are siblings from the second couple of this family. Both siblings displayed characteristics similar to each other and their cousins. Both were born after term, uncomplicated pregnancies with similar birth weights of 3270g. F2:V-8 presented with craniosynostosis of the coronal, sagittal and lambdoid sutures, while in F2:V-9 only the coronal suture was involved. A complex front orbital advancement was performed in the her. Both shared the typical craniofacial characteristics observed in other families including a coarse face, synophris, proptosis, long eyelashes, sagging cheeks, thick lips, prominent nose with convex nasal ridge, and broad nasal tip. F2:V-9 had a cleft soft palate with minor extension to the hard part, while his sister only had a highly arched palate. Skeletal abnormalities were the same in both sibs with brachydactyly, 5th finger clinodactyly and syndactyly of the 2nd, 3rd and 4th toe. Echocardiography was normal in F2:V-9 but not performed in F2:V-8. Both wore hearing aids for conductive hearing loss secondary to otitis media. F2:V-8 had optic nerve hypoplasia

and F2:V-9 had optic nerve atrophy with a visual acuity of 6/60. Cutis laxa and inguinal hernia were present in both siblings. In addition, F2:V-8 was diagnosed was left hydroureter and right duplex kidney.

In this family, homozygosity mapping showed a shared 22.9Mb homozygous region on chromosome 2 (20,605,248-43,530,418) between the affected individuals, which is absent in unaffected family members. NGS exome sequencing subsequently identified a homozygous nonsense *LTBP1* variant NM_206943.4: c.4431T>A (p.Cys1477*).

Family 3

Family 3 consists of a 1,6 year old boy (F3:II-1) and a 4 year old girl (F3:II-2) from a consanguineous family of Pakistani descent. The pregnancy of the first child was complicated by a vaginal bleeding. Both presented at the age of 6 months with craniosynostosis involving the right coronal and sagittal suture. The overall head shape was deformed and there was a 3th and 4th nerve palsy resulting in ptosis and squint. They displayed craniofacial features similar to our other families, with a coarse, long face, broad forehead, proptosis, arched eyebrows, sagging cheeks, microretrognathia, downslanting palpebral fissures, characteristic prominent nose (broad nasal bridge and tip), eyelashes and lips (thick upper and lower lip vermillion). In addition, protruding ears with large earlobes were observed. Both showed cutis laxa and deep palmar creases. F3:II-2 had a height of 95cm (P9; -1,36SD), weight of 14kg (P14; -1,09SD) and OFC of 48,5cm (P24; -0,71SD). Her arm span is 88cm, the pubis-ground distance 45cm and sitting height is 56cm. Her brother's length was 87cm (P90; +1,30SD), his weight 12kg (P54; +0,11SD) and his OFC 47cm (P25; -0,68SD). Skeletal features included brachydactyly, 5th finger clinodactyly, syndactyly of the 4th and 5th toes, joint hyperlaxity and genua vara. Heart auscultation revealed a loud P2, but echocardiography was not performed. Both display delayed developmental milestones with independent sitting age 12 months. Walking was achieved at ages 17 and 24 months, respectively. In the oldest sib, there was no evidence of any learning difficulties. Other clinical features included severe feeding problems, pallor and prune belly. In addition, F3:II-2 was diagnosed with moderate secundum atrial septal defect (ASD). ES identified a homozygous *LTBP1* frameshift variant resulting from a 5bp deletion (NM_206943.4: c.3991_3995del (p.Thr1331Asnfs*20)) in both siblings.

Family 4

Individual F4:II-1 is a 2 year old girl born to consanguineous parents of Saudi Arabic descent. She was born after an uneventful pregnancy at 39 weeks of gestation. At birth, marked craniofacial dysmorphism, craniosynostosis with hydropcephalus and cutis laxa were evident. The craniosynostosis involved a near complete fusion of the major sutures, involving the metopic, sagittal, coronal, lambdoid and squamosal suture. CT imaging of the skull showed a striking copper beaten appearance. The person received a ventriculoperitioneal shunt at the age of 2 months followed by successful corrective surgery at the age of one year. Clinical examination at the age of 21 months showed distinctive craniofacial features including a coarse face, sparse hair with low anterior hairline, long eyelashes, prominent eyes, broad nasal bridge and tip, a long and smooth philtrum, a tented upper lip with thick lower lip vermillion, protruding ears with overfolded helices, and hypotelorism. She presented with mild cutis laxa with prominent palmar creases, a distended abdomen and flat nipples. Skeletal abnormalities included short stature, a short thorax with pectus excavatum, clinodactyly, genua vara and hypermobile joints. An echocardiography performed at 21 months was normal, but she has history of a small ASD which was treated conservatively. She showed mild motor developmental delay with first independent sitting at the age of 13 months. A brain MRI showed normal major brain structures, but prominent Chiari I malformation and possible distal aqueduct stenosis. She had normal hearing and vision. She experiences some mild feeding difficulties due to poor appetite. A homozygous *LTBP1* nonsense (NM_206943.4: c.1342C>T, p.(Gln448*)) variant was identified.

Supplemental Data include 11 supplemental figures and 4 supplemental tables.

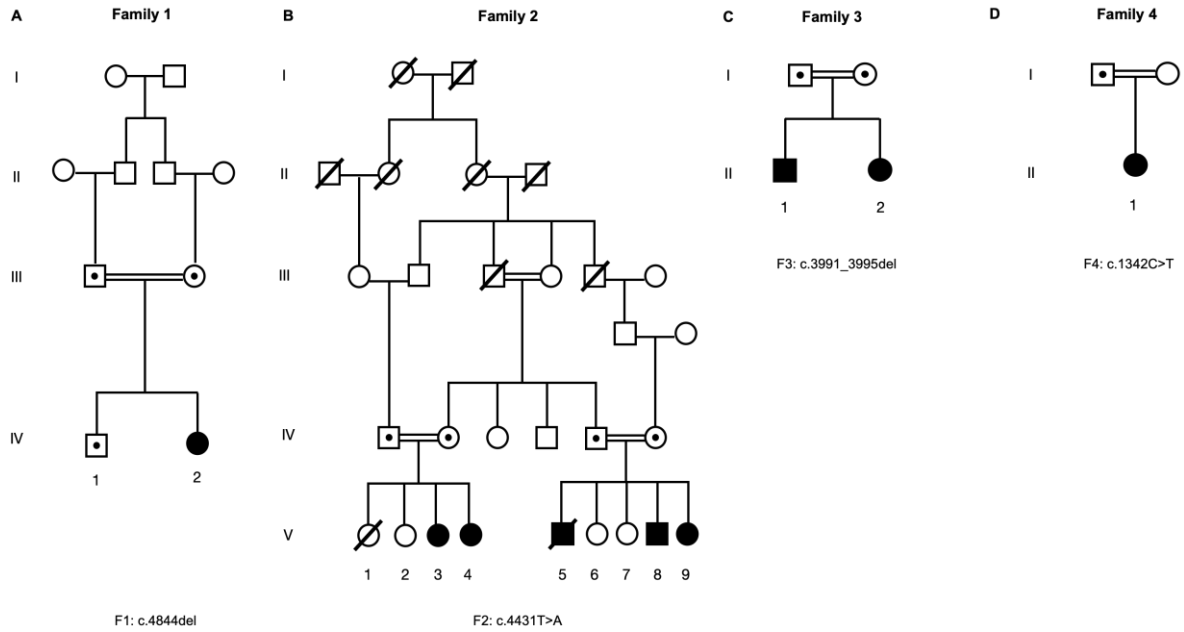

Figure S1: Pedigrees of the reported families. (A-D) Pedigree analysis of affected individuals in four unrelated consanguineous families carrying *LTBP1* variants confirms segregation of the variants with the phenotype.

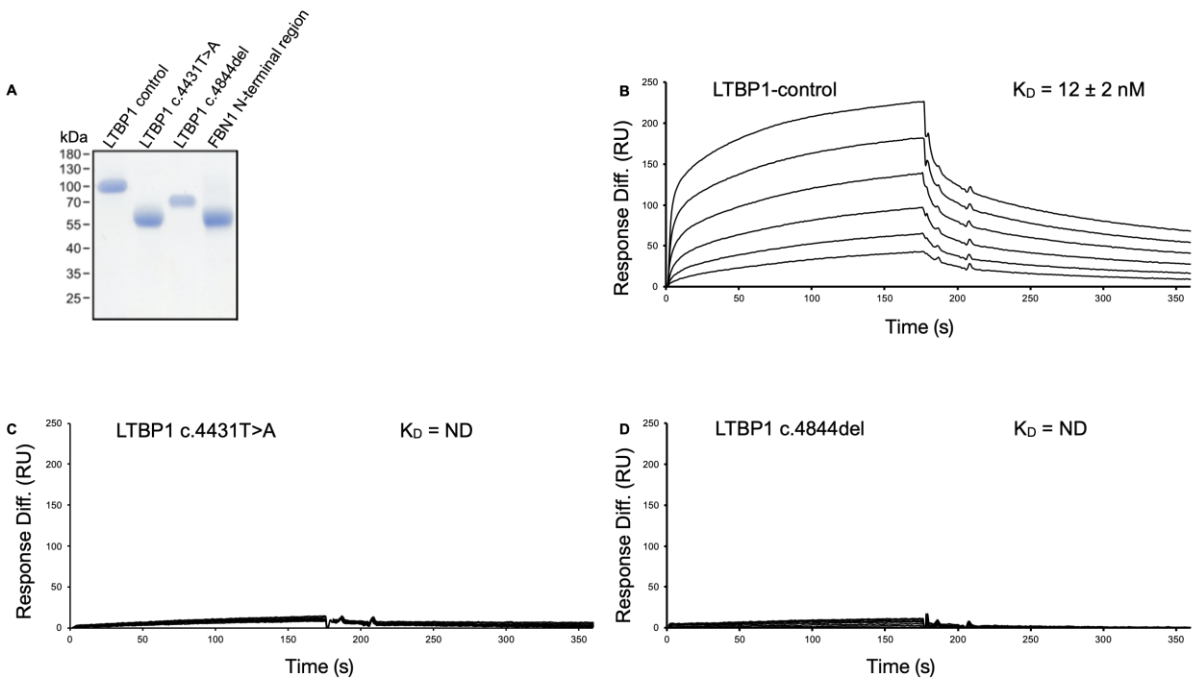

E

Fragment coated	Fragment incubated	KDs
LTBP1 control	FBN1 N-terminal region	9 ± 3 nM
LTBP1 c.4431T>A	FBN1 N-terminal region	108 ± 25 nM
LTBP1 c.4844del	FBN1 N-terminal region	69 ± 12 nM
LTBP1 control	FBN2 N-terminal region	6 ± 2 nM
LTBP1 c.4431T>A	FBN2 N-terminal region	234 ± 23 nM
LTBP1 c.4844del	FBN2 N-terminal region	94 ± 14 nM

Figure S2: Binding assays show reduced interaction between the N-terminal fibrillin-1 region and mutant C-terminal LTBP1 regions. (A) SDS/PAGE of recombinantly expressed and affinity purified C-terminal LTBP1 regions and the N-terminal region of FBN1. (B-D) SPR sensorgrams of the interaction between the C-terminal LTBP1 variants and control (flown over as soluble analyte) and N-terminal region of FBN1 (immobilized as ligands on sensor chip). ND. Not determinable. (E) Equilibrium dissociation constant solid-phase binding assay from C-terminal LTBP-1 regions carrying the c.4431T>A and c.4844del variants (immobilized) to fibrillin-1 and -2 proteins incubated in solution.

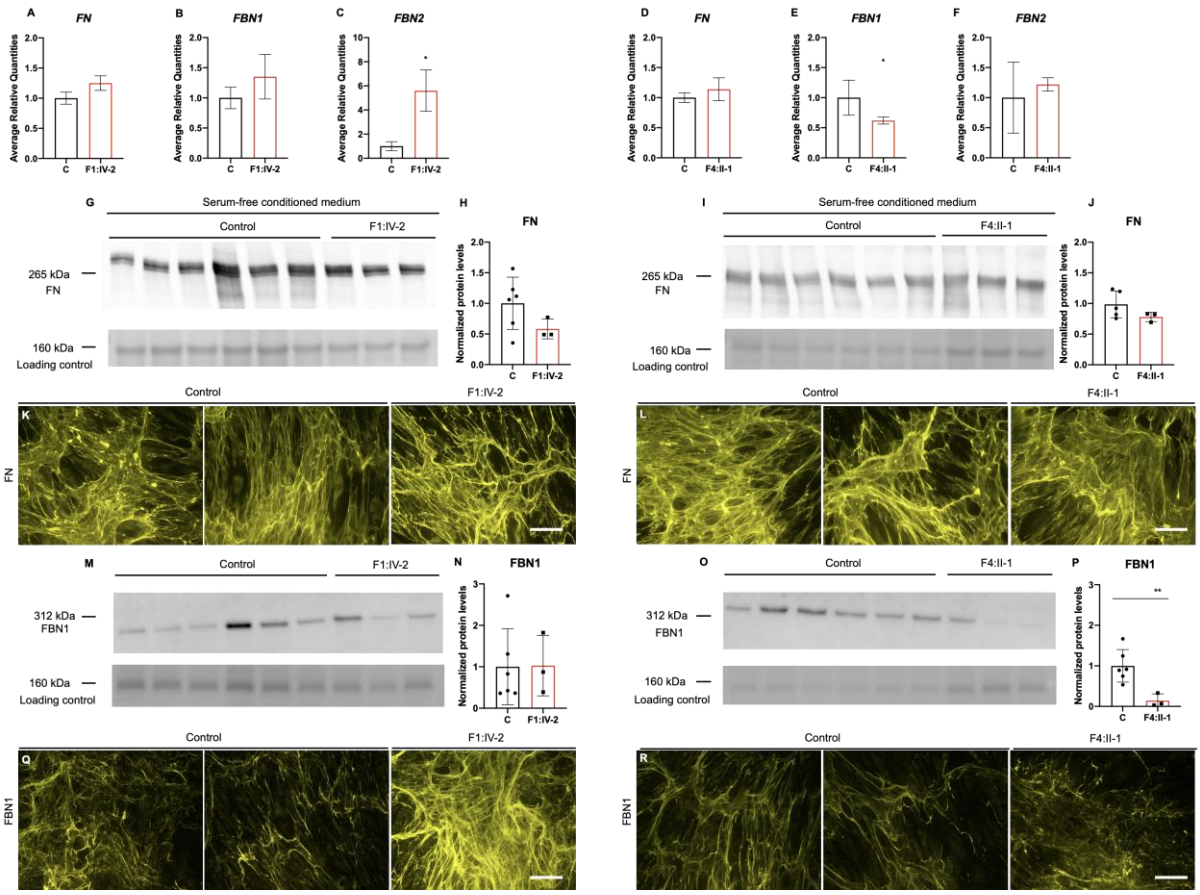

Figure S3: LTBP1 variants affect the fibrillin but not the fibronectin component of the ECM *in vitro*. (A-F) Quantification of *FN, FBN1* and *FBN2* gene expression dermal fibroblast cultures at 1 dpc derived from affected individuals F1:IV-2 and F4:II-1 and respective control subjects by RT-qPCR. (G,I,M,O) Immunoblot of 14 dpc conditioned media obtained from fibroblast cultures derived from individuals F1:IV-2 and F4:II-1 and respective gender- and age-matched control subjects. Specific antibodies were used to detect FN (G,I) and FBN1 (M,O), and imperial blue staining was used to monitor equal loading. (H,J,N,P) Quantification of protein expression of FN (H,J) and FBN1 (N,P) in conditioned media. (K,L,Q,R) Representative images of immunofluorescent analysis of FN (K,L) and FBN1 (Q,R) in 9 dpc fibroblast cultures derived from affected individuals F1:IV-2 and F4:II-1 and respective control subjects. Scale bar represents 50 µm. Data are expressed as mean ± standard deviation (SD). * P-value < 0.05, ** P-value < 0.01. Two-tailed unpaired t-test with Welch's correction was used for statistical analysis.

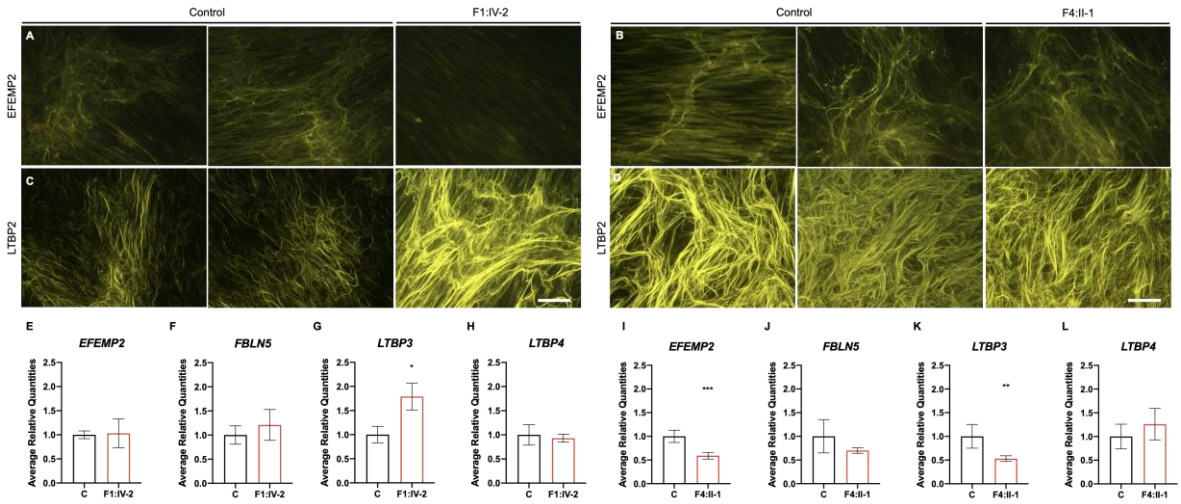

Figure S4: Specific *LTBP1* variants render different responses of adaptor proteins. (A,B) Representative images of immunofluorescent analysis of EFEMP2 in dermal fibroblast cultures derived from individuals F1:IV-2 in A and F4:II-1 in B and their respective control subjects at 9 dpc. (C,D) Representative images of immunofluorescent analysis of LTBP2 in dermal fibroblast cultures derived from individuals F1:IV-2 in C and F4:II-1 in D and their respective control subjects. Scale bar represents 50 µm. (E-L) Quantification of *EFEMP2*, *FBLN5*, *LTBP3*, and *LTBP4* gene expression in dermal fibroblast cultures at 1 dpc derived from affected individuals F1:IV-2 and F4:II-1 and respective control subjects by RT-qPCR. Data are expressed as mean ± SD. * P-value < 0.05, ** P-value <0.01, *** P-value <0.001. Two-tailed unpaired t-test with Welch's correction was used for statistical analysis.

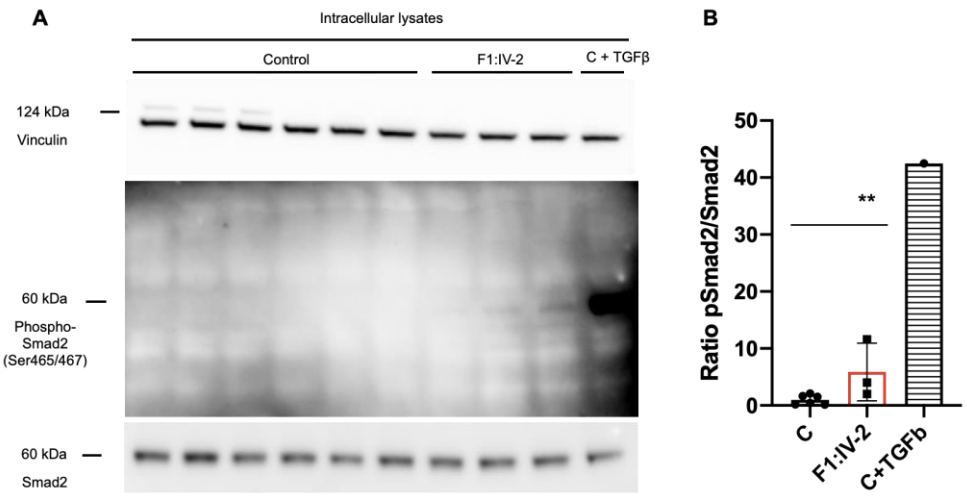

Figure S5: Immunoblot of (non-)phosphorylated Smad2 levels in F1:IV-2 and respective controls (repeat). (A) Immunoblot of intracellular lysates at 1 dpc obtained from fibroblast cultures derived from individual F1:IV-2 and respective sex- and age-matched control subjects. One of the control subjects was stimulated with TGFβ as positive control. (B) Band intensities of chemiluminescent signals of non-phosphorylated and phosphorylated Smad2 were quantified with ImageJ. The ratio pSmad2 to Smad2 was normalized to fibroblast cultures derived from sex- and age-matched control subjects. Vinculin was used as loading control. Data are expressed as mean ± SD. ** P-value <0.01. Two-tailed unpaired t-test with Welch's correction was used for statistical analysis.

```
XP_017207300.1 DAGFVSTRTG- - CQDVDECSLNENTCGSHGTCQNTI GSF I CQCDPGFKDSQDGQGCVDVN
NP_996826.3    QQGFSISADGRTCEDI  DEC -VNNTVCDSHGFCDNTAGSFRCLCYQGFQAPQDGQGCVDVN
NP_000618.4    QQGFSISADGRTCEDI  DEC -VNNTVCDSHGFCDNTAGSFRCLCYQGFQAPQDGQGCVDVN
                :  ** :   *   *:*:***  :*: ..*. *** *  *:** * **  * *   **:  .** * *******

XP_017207300.1 ECELLGNVCGEATCENREGTFLCLCPDD LQEFDPMLGKC I STPPVT - - - - - - - - TVERKE
NP_996826.3    ECELLSGVCGEAFCENVEGSFLCVCADENQEYSPMTGQCRSRTSTDLDVDVDQPKEEKKE
NP_000618.4    ECELLSGVCGEAFCENVEGSFLCVCADENQEYSPMTGQCRSRTSTDLDVDVDQPKEEKKE
                ******. .******. ***  **:***: *.*:  **.: **  *: * *  . .  .  *.**

                                    ✂➔ Ltbp1-/-Δ29

XP_017207300.1 CYFNLNDENLCDKVLASSMTKEECCCTLGA|GWGDNCEVHPCPIPGTDQFSQMCPAGRGYL
NP_996826.3    CYYNLNDASLCDNVLAPNVTKQECCCTSGV|GWGDNCEI FPCPVLGTAEFTEMCPKGKGFV
NP_000618.4    CYYNLNDASLCDNVLAPNVTKQECCCTSGV|GWGDNCEI FPCPVLGTAEFTEMCPKGKGFV
                * *:**** .***:***. . : **:* **** *. * *** ***:.***:  ** : *::*.**  *. *::

XP_017207300.1 I SGDPMSTTSS LAENTKADADECQLFGSEICKDGFCLNTAGWYECYCKSGLYYDESKLQC
NP_996826.3    PAGE- -  SSSEAGGENYK-DADECLLFGQEICKNGFCLNTRPGYECYCKQGTYYDPVKLQC
NP_000618.4    PAGE- -  SSSEAGGENYK-DADECLLFGQEICKNGFCLNTRPGYECYCKQGTYYDPVKLQC
                 :* :   *: : :   .**  ***** * ***. ***: ******    ****** . * * **.  * ***

XP_017207300.1 LDTDECQDEAKCRDGECMNTYGSYQCFCTPPMVLAMDNTHCILPDVAGQS--EADLYSGV
NP_996826.3    FDMDECQDPSSCIDGQCVNTEGSYNCFCTHPMVLDASEKRCIRPAESNEQ IEETDVYQDL
NP_000618.4    FDMDECQDPSSCIDGQCVNTEGSYNCFCTHPMVLDASEKRCIRPAESNEQ IEETDVYQDL
                : *. **** *  :.* * *: *:**  *** :**** ** **  .:. .** *   :.:  .  *:*: * ..:

XP_017207300.1 CWERVTENFSCANPI PN IHTSFTECCCLYGEAWGNDCALCPGKNTDSYAQMCNI - - - - - R
NP_996826.3    CWEHLSDEYVCSRPLVGKQTTYTECCCLYGEAWGMQCALCPLKDSDDYAQLCNIPVTGRR
NP_000618.4    CWEHLSDEYVCSRPLVGKQTTYTECCCLYGEAWGMQCALCPLKDSDDYAQLCNIPVTGRR
                ** * .::: : :  *:.*:  .  :*::********** * *  :***** *: :*. ***:***      *

                                                    Ltbp1-/-Δ35 ➔✂

XP_017207300.1 RPYGRDALVAGPIGVSPDYNPQPLNPDGTLPYIEDYDEPRNPYDAFEGLRAEE|CGVLNGC
NP_996826.3    QPYGRDALV - - - - - - - - DFSEQ - YTPEADPYFIQD- - - - - RF LNSFEELQAEE|CG I LNGC
NP_000618.4    QPYGRDALV - - - - - - - - DFSEQ - YTPEADPYFIQD- - - - - RF LNSFEELQAEE|CG I LNGC
                .**** ****          *:.  *   .* :.  : *:*       .  : :** *. *** ** :*** *

XP_017207300.1 ENGRCVRVQEGYTCDCFDGYTLDMSRMACVDINECSELNAKMSLCKNGNCINTQGSYKCV
NP_996826.3    ENGRCVRVQEGYTCDCFDGYHLDTAKMTCVDVNECDELNNRMSLCKNAKCINTDGSYKCL
NP_000618.4    ENGRCVRVQEGYTCDCFDGYHLDTAKMTCVDVNECDELNNRMSLCKNAKCINTDGSYKCL
```

```
                ** ****** *********** *  **  : .*:* **:** *.***  .* *****.:****:*****:

XP_017207300.1 CLPG FILSAQHNYCVPHRQN - - - ATSTGTE
NP_996826.3    CLPGYVPSDKPNYCTPL NTA LNLEKDSDLE
NP_000618.4    CLPGYVPSDKPNYCTPL NTA LNLEKDSDLE
                **** : :  *  :  *** .*   .          . . : .  *
```

Figure S6: Amino acid sequence alignment of LTBP1 between *H. Sapiens* and *D. rerio*. C-terminal amino acid sequence alignment (Clustal Omega) between *H. sapiens* LTBP-1S precursor [NCBI:NP_000618.4], *H. sapiens* LTBP-1L precursor [NCBI:NP_996826.3] and *D. rerio* Ltbp1 [NCBI:XP_017207300.1] starting from cb EGF-like domain 13. Cb EGF-like domains in *H. sapiens* are highlighted in blue and predicted to be conserved in *D. rerio*. EGF-like domains in *H. sapiens* are highlighted in yellow and predicted to be conserved in *D. rerio*. TGFβ-binding domains in *H. sapiens* are highlighted in red and predicted to be conserved in *D. rerio*. Conservation of amino acid sequences are shown below the alignment: "*" means residues identical in all sequences in the alignment; ":" means conserved substitutions; "." means semi-conserved substitutions; space means no conservation. Note that *ltbp1*$^{-/-}$Δ29 zebrafish is lacking 6 domains: 2 predicted TGFβ-binding domains, 3 predicted cb EGF-like domains, and 1 EGF-like domain. *Ltbp1*$^{-/-}$Δ35 zebrafish is lacking 2 domains: 1 predicted cb EGF-like domains, and 1 EGF-like domain.

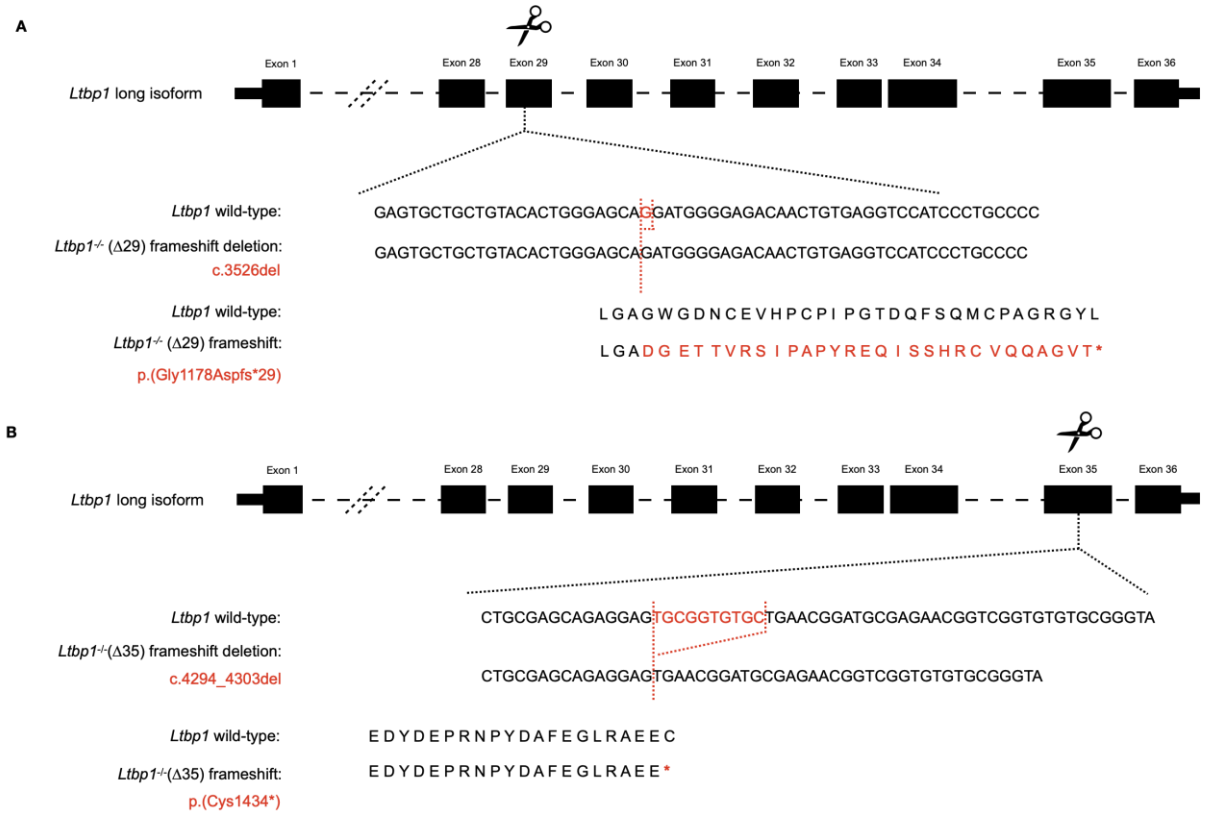

Figure S7: Schematic illustration of the targeting strategy for the generation of *Itbp1*$^{-/-}$*Δ29* and *Itbp1*$^{-/-}$*Δ35* zebrafish. (A) A frameshift-inducing 1 bp deletion (c.3526del) was generated in exon 29 of the zebrafish *ltbp1* gene using CRISPR-Cas9 technology. The deleted nucleotides are marked in red. The frameshift was predicted to cause premature translation termination p.(Gly1178Aspfs*29). The termination codon (red asterisk) is indicated in the predicted mutated protein sequence. (B) A 10 bp frameshift-inducing deletion (c.4294_4303del) was introduced in exon 35 of the zebrafish *ltbp1* gene using CRISPR-Cas9. The deleted nucleotides are marked in red. The frameshift was predicted to cause premature translation termination (p.Cys1434*). The termination codon is shown in the predicted mutated protein sequence. Nucleotide RefSeq accession number *D. rerio ltbp1* [NCBI: XM_017351811.2]. Protein RefSeq accession number *D. rerio* Ltbp1 [NCBI: XP_017207300.1]. The *D. rerio ltbp1* gene resides on chromosome 17, spans a region of 160 kb and has not been duplicated during teleost evolution.

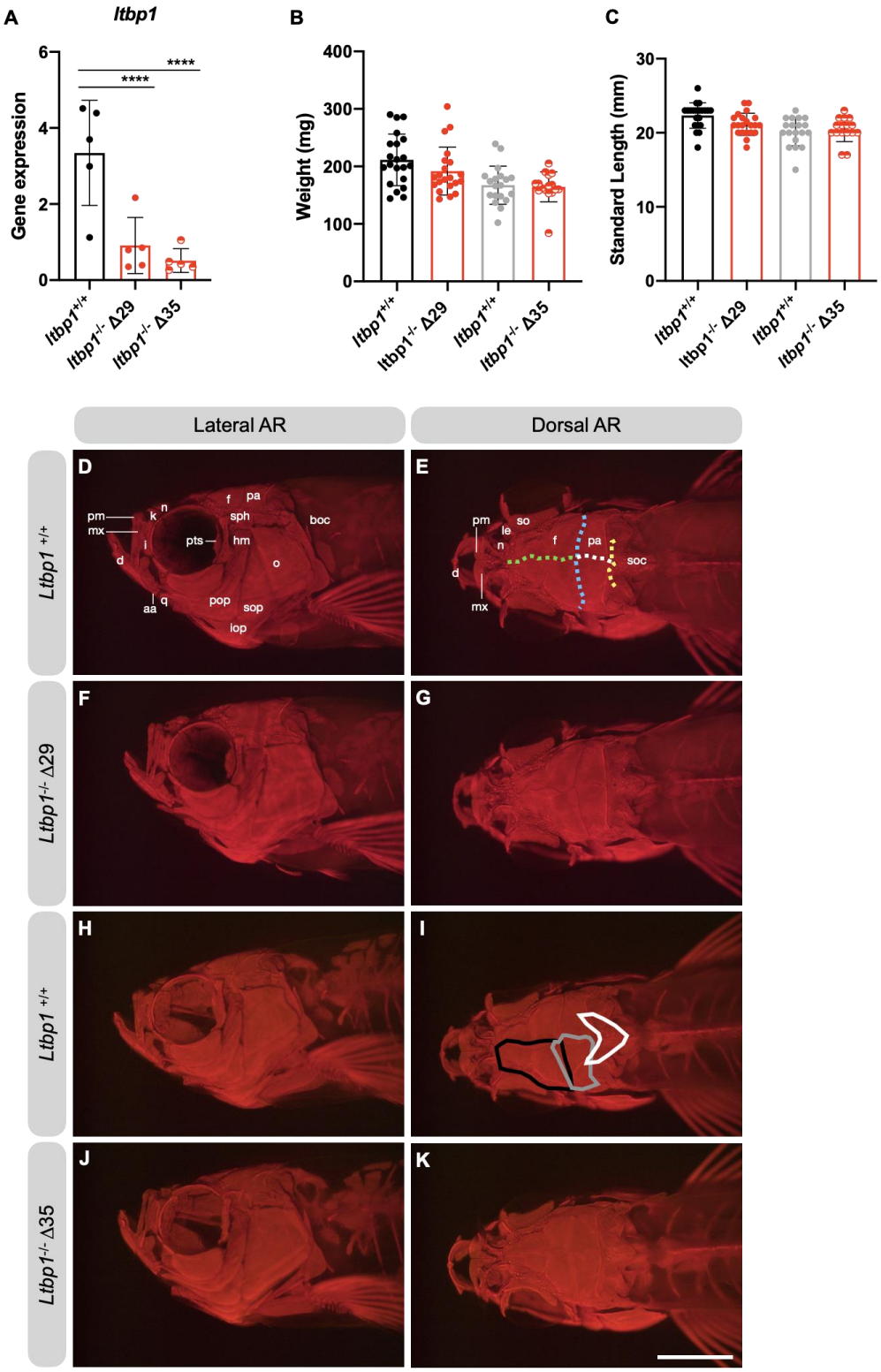

Figure S8: Adult morphological and craniofacial analysis of *ltbp1*$^{-/-}$*Δ29* and *ltbp1*$^{-/-}$*Δ35* zebrafish.

(A) *Ltbp1* mRNA levels in *ltbp1*$^{-/-}$Δ29 and *ltbp1*$^{-/-}$Δ35 zebrafish models at 15 dpf specified by RT-qPCR. *Ltbp1*$^{-/-}$Δ29 and *ltbp1*$^{-/-}$Δ35 zebrafish had a similar standard length (B) and weight (C) compared to WT siblings at 4 months of age. Representative lateral (D, F, H, J) and dorsal (E, G, I, K) images of adult

cranium stained for mineralized bone with Alizarin Red. Interfrontal suture (green dashed line), coronal suture (blue dashed line), sagittal suture (white dashed line) and lambdoid suture (yellow dashed line) are indicated in E. Frontal (black line), parietal (grey line), and supraoccipital bone (white line) are shown in I. Note that in contrast to humans, the sutures are overlapping in the calvaria of zebrafish. aa: anguloarticular; boc: basioccipital; f: frontal; hm: hyomandibula; i: infraorbital 1; iop: interoperculum; k: kinethmoid; le: lateral ethmoid; mx: maxilla; n: nasal; o: operculum; pa: parietal; pm: premaxilla; pop: preoperculum; pts: pterosphenoid; q: quadrate; so: supraorbital; soc: supraoccipital; sop: suboperculum; sph: sphenotic. Data are expressed as mean ± standard deviation (SD). **** P-value <0.0001. One-way ANOVA was used for statistical analysis in A. Two-tailed unpaired t-test was used for statistical analysis in B and C.

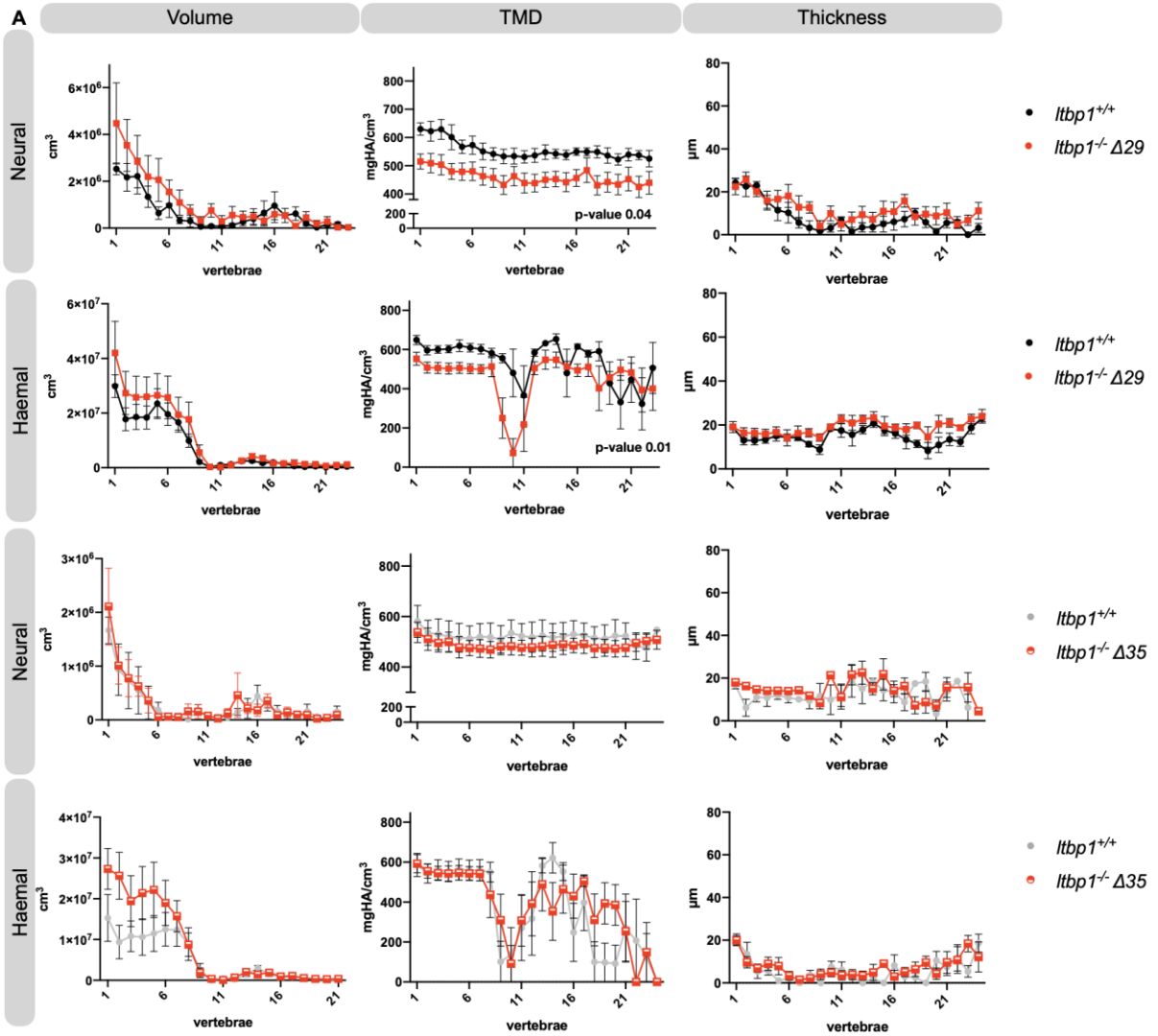

Figure S9: Loss of both *ltbp1* isoforms in zebrafish causes hypo-mineralization of the neural and haemal associated vertebral elements. (A) Quantitative µCT analysis of the vertebral column in five *ltbp1*$^{-/-}$Δ29 zebrafish versus five WT siblings and five *ltbp1*$^{-/-}$*Δ35* zebrafish versus four WT siblings at the age of four months. The bone volume, TMD and bone thickness was calculated from the neural associated element (neural arch and neural spine) and the haemal associated element (haemal arch and haemal spine). The X-axis represents each abdominal and caudal vertebral body along the anterior-posterior axis. Data are presented as mean ± standard error of the mean (SEM). Data were analyzed in the R statistical environment.

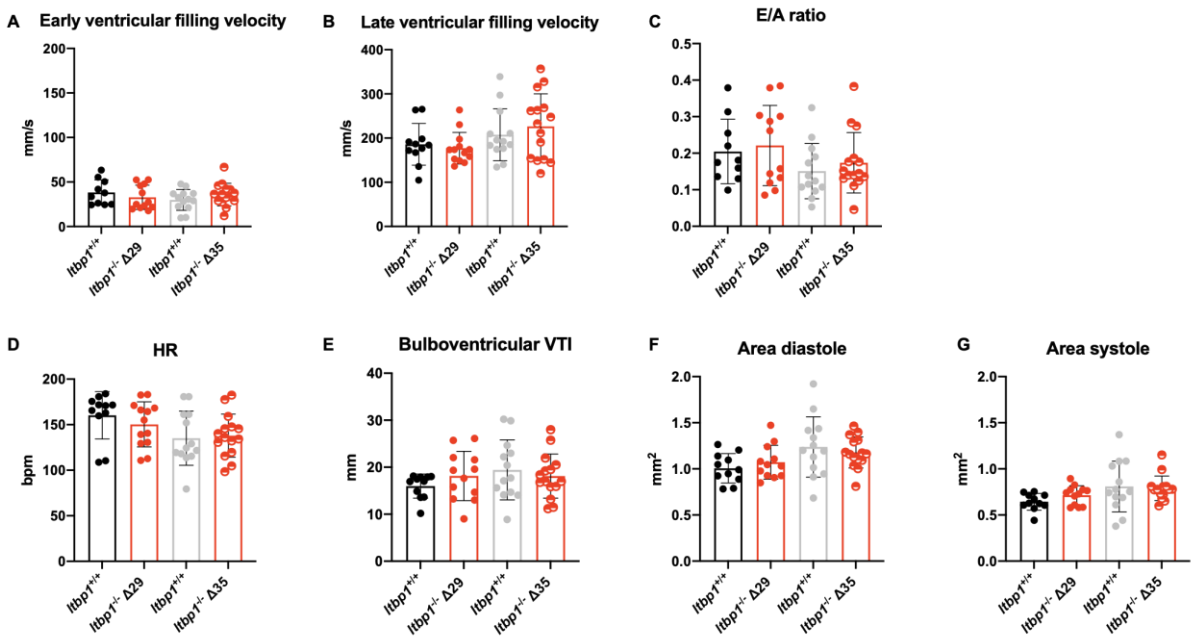

Figure S10: (A-G) Parameters obtained from cardiac ultrasound examination of 10-months old *ltbp1*$^{-/-}$ Δ29 and *ltbp1*$^{-/-}$Δ35 zebrafish and their respective WT siblings. A: late ventricular filling velocity; bpm: beats per minute; E: early ventricular filling velocity; VTI: velocity time integral. Note that the ventricular outflow is measured during ventricular systole through the bulboventricular valve of the zebrafish heart (similar structure to the aortic valve in humans). Data are expressed as mean ± SD. Two-tailed unpaired t-test was used for statistical analysis.

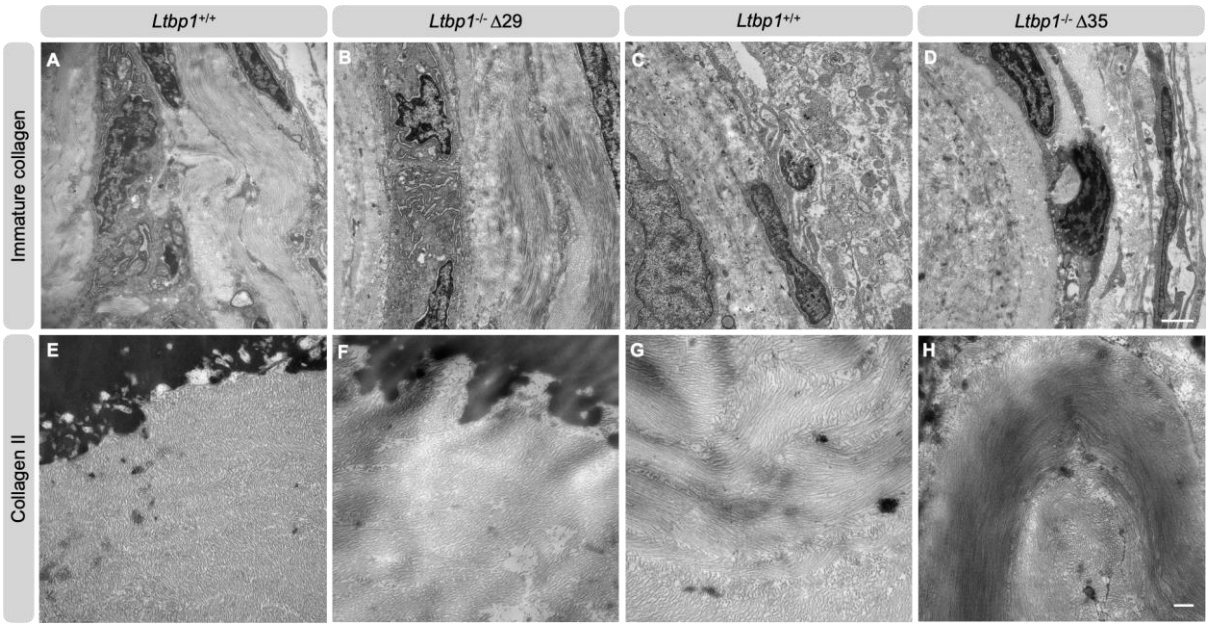

Figure S11: Ultrastructural analysis of immature collagen and collagen 2 in the intervertebral ligament of adult *ltbp1* mutant and WT zebrafish. (A-D) Representative images of ultrathin sagittal sections showing internal immature collagen structures of zebrafish intervertebral ligament of 4-6 months old adult *ltbp1*$^{-/-}$Δ29 and *ltbp1*$^{-/-}$Δ35 zebrafish and WT siblings. (E-H) Representative images of ultrathin sagittal sections showing internal immature collagen structures of zebrafish intervertebral ligament of 4-6 months old adult *ltbp1*$^{-/-}$Δ29 and *ltbp1*$^{-/-}$Δ35 zebrafish and WT siblings. Scale = 1 µm in A-D, scale = 200 nm in E-H.

Dermal fibroblast	Age (years)	Sex
Control 1	25	female
Control 2	25	female
F1:IV-2	9	female
Control 3	2	male
Control 4	2	male
F4:II-1	1.6	male

Table S2: LTBP1 mutant and control dermal fibroblasts used in this study

Gene Symbol	Forward primer sequence	Reverse primer sequence
YWHAZ	ACTTTTGGTACATTGTGGCTT	CCCCCAGGACAAACCAGTAT
HPRT1	TGACACTGGCAAAACAATGCA	GGTCCTTTTCACCAGCAAGCTA
***LTBP1* F1**	TGCTGGGAACATCTGAGTGA	CTGAGCATAGTCATCTGAATCCTT
***LTBP1* F4**	AAGGGGATTTCAGGAGAGCAG	CAGGTCACTTTACAGATGCTCG
EFEMP2	GCCCGAGTGTGTGGACAT	CAACACAGGAGCGGTTGTTA
FBLN5	TGGATGAAAGCAACCAATGTGT	CAATATCCGTCGGTGCAGGA
LTBP3	GATCGCTCCCACTCAGGTC	TTGCAGTGGCAGGAGTAGT
LTBP4	GCCTCTGTGACCAGGGTT	ATTTTCACACAGGGCAGCTC
FBN2	AACCGCTGTGCTTGTGTTTAT	TCTGGTTGTTGACCTGAGTGA
FN	GAACAAACACTAATGTTAATTGCCCA	GAGACATGCTTGTTCCTCTGG
LOX	TATGGCTACCACAGGCGATTT	GTCTGCACCATAGGTATCATAACA
COL1A1	GTACAGAACGGCCTCAG	GTTCTTGGTCTCGTCACA
COL1A2	CCTAACCAAGGATCGACTAT	GCCATTTCCTTGGAAGTCA
COL3A1	GAGGATGGTTGCACGAAACA	TGATCAGGACCACCAATGTCA
POSTN	TCTGTGCCCTTCAACAGATTTT	GCAGCCTTTCATTCCTTCCATT
CTGF	GGTTACCAATGACAACGCCT	GATGCACTTTTTGCCCTTCTTAAT
SERPIN1	GATTCAAGATTGATGACAAGGGC	TGTGGTGCTGATCTCATCCTT
ltbp1	ATACACCTGTGACTGCTTCGAT	AGCTCGGAGCATTCGTTGATA

Table S3: Primer sequences for qPCR analysis

Zebrafish line	Forward primer sequence	Reverse primer sequence
***ltbp1*$^{-/-}$Δ29**	GGCAGCGTACATCTCCAAAT	TTTCTCTCCTGCCAGATCGT

***ltbp1*$^{-/-}$Δ35**	ACTTGCTTTAAACCCCTCTGTC	TCTGCCTGCAGCTTTTCTCA

Table S4: Primer sequences for genotyping